Proceedings of the 55th Israel Annual Conference
on Aerospace Sciences, Tel-Aviv & Haifa, Israel,
February 25-26, 2015

Distance-Constrained Formation Tracking Control

Oshri Rozenheck[1], Shiyu Zhao[2], and Daniel Zelazo[2*†]

This work considers a multi-agent formation control problem where a designated leader is subjected to an additional velocity reference command. The entire formation should follow the leader while maintaining the inter-agent distance constraints. By introducing a proportional control gain term to a gradient controller that stabilizes infinitesimally rigid formations, we are able to prove stability of the formation error dynamics with velocity input while ensuring that the steady state formation error is bounded. Upper bounds on the steady-state error are also given in terms of properties of the specified formation. Numerical simulations are shown to illustrate the theoretical results.

I. Introduction

Formation control of multi-robot networks is an area of ongoing research in control systems. In recent years, there has been an increasing number of contributions dealing with the control of multiple agent formations. Of the many control strategies for formation control, distance-constrained formation stabilization has been extensively studied [1–9]. A closely related problem is formation tracking where the objective is to find a control scheme that allow multiple robots to maintain some given formation while executing additional tasks such as velocity tracking or leader following.

The words 'move as a formation' have the usual meaning of everyday language: the formation at one instant of time is congruent to the formation at another instant of time, or equivalently, all inter-agent distances are preserved over all time. Distance-constrained formation control aims at maintaining inter-agent distances and utilizes relative measurements (i.e., distances and relative-positions) to generate the control action. The theory of rigidity has emerged as the correct mathematical foundation for defining distance-constrained formations and proving that distance-constrained formation control strategies are stabilizing [3, 10, 11]. In [12], application of the center manifold theorem was used to prove the local stability of infinitesimally rigid formations. Lyapunov-based approaches were employed in [6, 13]. As a first contribution of our work, we provide an alternative local stability proof by deriving the dynamics of the formation error and employing Lyapunov's indirect method.

Although some earlier related studies addressed the issues of analyzing the decentralized control laws embedded in the agents for distance control, fewer can be found answering the question of tracking an input reference of only one of the agents. In [14, 15] different methods are used including a coordinated control approach and a combination of consensus-based controllers with the cascaded approach to control agents with unicycle dynamics. The aid of one or more virtual agents to help the formation achieve a desired common velocity or to arrive at a desired destination is considered in [16–18]. In particular, [19] proposed a flocking algorithm

*[1]O. Rozenheck is with the Technion Autonomous Systems Program, Technion - Israel Institute of Technology, Haifa, Israel. oshriroz@tx.technion.ac.il

†[2]S. Zhao, and D. Zelazo are with the Faculty of Aerospace Engineering, Technion - Israel Institute of Technology, Haifa, Israel. szhao@tx.technion.ac.il, dzelazo@technion.ac.il

with a virtual leader by including a navigational feedback mechanism to every agent under the assumption that all agents are being informed. In [6, 18, 20], the formation tracking problem is considered for agents with second-order dynamics.

In this paper, we investigate the problem of controlling a group of mobile agents with single integrator dynamics to track a reference velocity of a single leader. When one of the agents is assigned with an external velocity command, the objective is to preserve the correct distance-constrainted formation by the other agents while following the leader. In the absence of any additional control action, the standard rigidity based formation stabilization solutions will exhibit a steady-state formation error. Our approach is to combine gradient control laws with a proportional (P) gain controller to reduce this steady-state error. We show that such a scheme preserves the stability properties of the formation error dynamics as well as properties of the networked system's centroid. We also reveal more interesting relations between the upper bound of the steady state error and the graph properties. This scheme has many advantages, including a simple and distributed implementation and no need for virtual leaders.

The paper is organized as follows. An overview on rigidity theory is provided in Section II. The distance-constrained formation control law and stability analysis is reviewed in Section III. The proportional formation controller with stability and performance analysis is presented in Section IV. Numerical simulations are provided in Section V to illustrate the theoretical results. Section VI contains concluding remarks and areas for future work.

II. Preliminaries

A. Notations

Given $A_1, \ldots, A_n \in \mathbb{R}^{p\times q}$, when the range of i is clear from the context, denote $\mathrm{diag}(A_i) \triangleq \mathrm{blkdiag}\{A_1, \ldots, A_n\} \in \mathbb{R}^{np\times nq}$. Denote I_n as the $n\times n$ identity matrix. Let $\mathbf{1}_n = [1, \ldots, 1]^{\mathrm{T}} \in \mathbb{R}^n$ be the vectors of all ones. The eigenvalues of a symmetric positive semi-definite matrix A are denoted as $0 \leq \lambda_1(A) \leq \lambda_2(A) \leq \cdots \leq \lambda_n(A)$.

B. Graph Theory

An *undirected graph* $\mathcal{G} = (\mathcal{V}, \mathcal{E})$ consists of a vertex set $\mathcal{V}$ and an edge set $\mathcal{E} \subseteq \mathcal{V} \times \mathcal{V}$, where an edge $\{i, j\}$ is an unordered pair of distinct nodes i and j. We denote the number of nodes in a graph as $n \triangleq |\mathcal{V}|$ and the number of edges as $m \triangleq |\mathcal{E}|$. If $\{i, j\} \in \mathcal{E}$, then i and j are said to be *adjacent*; this is also denoted as $i \sim j$. The degree of vertex i, deg_i, is the cardinality of the set of vertices adjacent to it. The set of neighbors of vertex i is denoted as $\mathcal{N}_i \triangleq \{j \in \mathcal{V} : \ \{i, j\} \in \mathcal{E}\}$. A *spanning tree* is a connected graph with $|\mathcal{V}| - 1$ edges. An *orientation* of an undirected graph is the assignment of a direction to each edge. An *oriented graph* is an undirected graph together with a particular orientation. The *incidence matrix* $E \in \mathbb{R}^{n\times m}$ of an oriented graph is the $\{0, \pm 1\}$ matrix with rows indexed by vertices and columns by edges. For any connected graph, the incidence matrix satisfies $\mathrm{Null}\,(E^{\mathrm{T}}) = \mathrm{span}\{\mathbf{1}_n\}$ [21]. The Laplacian of $\mathcal{G}$, $L(\mathcal{G}) := E(\mathcal{G})E(\mathcal{G})^T$, is a rank deficient positive semi-definite matrix. The real spectrum of the Laplacian can thereby be ordered as $0 = \lambda_1(L(\mathcal{G})) \leq \lambda_2(L(\mathcal{G})) \leq ... \leq \lambda_n(L(\mathcal{G}))$. The multiplicity of the zero eigenvalue of the graph Laplacian is equal to the number of connected components of the graph [21]. Moreover, the second smallest eigenvalue of $L(\mathcal{G})$, $\lambda_2(L(\mathcal{G}))$ is also known as the algebraic connectivity of the graph.

C. Rigidity Theory

Rigidity theory plays an important role in distance-based formation control. We next review some important definitions and results from rigidity theory; for a more detailed review, see [3, 10].

A d-dimensional *configuration* is a finite collection of n points, $x = [x_1^{\mathrm{T}}, \ldots, x_n^{\mathrm{T}}]^{\mathrm{T}} \in \mathbb{R}^{2n}$, where $x_i \in \mathbb{R}^2$ and $x_i \neq x_j$ for all $i \neq j$. A *framework*, denoted as $\mathcal{G}(x)$, is an undirected graph $\mathcal{G}$ together with a configuration x, where vertex i in the graph is mapped to the point x_i. It is often useful to work with oriented graphs. Suppose $\{i, j\} \in \mathcal{E}$ corresponds to the kth directed edge in an oriented graph and define the edge vectors for a framework, sometimes called the relative position vector, as $e_k \triangleq x_j - x_i$. The edge vectors of the entire framework can be denoted as $e = \begin{bmatrix} e_1^{\mathrm{T}} \cdots e_m^{\mathrm{T}} \end{bmatrix}^{\mathrm{T}} \in \mathbb{R}^{2m}$.

Two frameworks $\mathcal{G}(x)$ and $\mathcal{G}(y)$ in $\mathbb{R}^2$ are *equivalent* if $\|x_i - x_j\| = \|y_i - y_j\|$ for all $\{(i, j)\} \in \mathcal{E}$. Two frameworks $\mathcal{G}(x)$ and $\mathcal{G}(y)$ in $\mathbb{R}^2$ are *congruent* if $\|x_i - x_j\| = \|y_i - y_j\|$ for all $i, j \in \mathcal{V}$. A framework $\mathcal{G}(x)$ is *globally rigid* if every framework that is equivalent to $\mathcal{G}(x)$ is also congruent to $\mathcal{G}(x)$. A framework $\mathcal{G}(x)$ is *rigid* if there exists an $\epsilon > 0$ such that if framework $\mathcal{G}(y)$ is equivalent to $\mathcal{G}(x)$ and satisfies $\|y_i - x_i\| \leq \epsilon$ for all $i \in \mathcal{V}$, then $\mathcal{G}(y)$ is congruent to $\mathcal{G}(x)$.

Given an arbitrary oriented graph, consider a framework $\mathcal{G}(x)$ with the edge vectors as $\{e_k\}_{k=1}^m$. Define the *edge function*, $F : \mathbb{R}^{2n} \times \mathcal{G} \to \mathbb{R}^m$ as

$$F(x, \mathcal{G}) \triangleq [\|e_1\|^2, \ldots, \|e_m\|^2]^{\mathrm{T}}.$$

The *rigidity matrix* $R(x)$ associated with a framework $\mathcal{G}(x)$ is the Jacobian of the edge function, $R(x) \triangleq \partial F(x, \mathcal{G})/\partial x \in \mathbb{R}^{m \times 2n}$. More specifically, if the i-th undirected edge is $\{j, k\}$, then the i-th row of $R(x)$ is defined as

$$\begin{array}{cccccc} & & j\text{th vertex} & & k\text{th vertex} & \\ [\cdots 0 \cdots & x_j^{\mathrm{T}} - x_k^{\mathrm{T}} & \cdots 0 \cdots & x_k^{\mathrm{T}} - x_j^{\mathrm{T}} & \cdots 0 \cdots]. \end{array}$$

A short calculation shows that $R(x)$ can be equivalently written as

$$R(x) = \mathrm{diag}(e_i^{\mathrm{T}})(E^{\mathrm{T}} \otimes I_2). \tag{1}$$

The *symmetric rigidity matrix* associated with a framework $\mathcal{G}(x)$ is the $2n \times 2n$ matrix defined as $\mathcal{R}(x) \triangleq R(x)^{\mathrm{T}} R(x)$ [2].

If dx satisfies $R(x)dx = 0$, then dx is called an *infinitesimal flex* of $\mathcal{G}(x)$. Framework $\mathcal{G}(x)$ is *infinitesimally rigid* if the only infinitesimal flexes are trivial, i.e., are the rigid body rotations and translations of the framework. A framework $\mathcal{G}(x)$ is *minimally infinitesimally rigid* (MIR) if it is infinitesimally rigid and the number of edges is $m = 2n - 3$. The following is the necessary and sufficient condition for infinitesimal rigidity.

Lemma 1. *([22]) A framework $\mathcal{G}(x)$ is infinitesimally rigid if and only if $rank(R(x)) = 2n-3$.*

Since there are $2n - 3$ edges in an MIR framework, the number of rows of the rigidity matrix must also be $2n - 3$, leading to the following corollary.

Corollary 1. *If a framework is MIR, then the rigidity matrix $R(x)$ has full row rank.*

Corollary 1 gives a sufficient condition for the rigidity matrix of a framework having full row rank. It is notable that there exist other frameworks that may not even be rigid possessing rigidity matrices of full row rank. For example, the rigidity matrix of a tree framework always has full row rank regardless of the configuration of the framework [23]. The notion of MIR frameworks and Corollary 1 turn out to be an important property for deriving the stability of distance-constrained formation problems.

III. Distance-Constrained Formation Stabilization

In this section, we first review a gradient control law for distance-constrained formation problems [12]. A contribution of this section is to derive an associated dynamical system based on the formation error. We then provide an alternative stability proof using the error dynamics and Lyapunov's indirect method.

Consider n ($n \geq 2$) agents, modeled as kinematic point masses, moving in a 2-dimensional Euclidean space. The motion of the agents are modeled as first-order integrators,

$$\dot{x}_i(t) = u_i(t), \quad i = 1, \ldots, n,$$

where $x_i(t) \in \mathbb{R}^2$ is the position of the i-th robot and $u_i(t) \in \mathbb{R}^2$ denotes the control input. To simplify notations, the time variable in $x(t)$ and $u(t)$ will be omitted (i.e., $x(t) := x$).

A formation can be defined by specifying the distances between pairs of agents in the system. Denote d_k as the desired distance between agent i and j for edge number k, $\{i, j\} \in \mathcal{E}$, and let $d = \begin{bmatrix} d_1^2 & \cdots & d_m^2 \end{bmatrix}^{\mathrm{T}} \in \mathbb{R}^m$ represent the *distance constraint vector*.

The *distance error*, $\delta \in \mathbb{R}^m$, is defined as the difference between the measured relative distances and the desired inter-agent distances,

$$\delta_k = \|e_k\|^2 - d_k^2, \quad k \in \{1, \ldots, m\}. \tag{2}$$

In [12], a gradient control law was proposed to locally and asymptotically stabilize infinitesimally rigid formations. The associated positive semi-definite potential function is defined as

$$\Phi(e) = \frac{1}{2} \sum_{k=1}^{m} \left(\|e_k\|^2 - d_k^2 \right)^2 = \frac{1}{2} \sum_{k=1}^{m} \delta_k^2. \tag{3}$$

Observe that $\Phi(e) = 0$ if and only if $\|e_k\|^2 = d_k^2$, $k = 1, \ldots, m$. The control for each agent is then taken as the gradient of the potential function (3),

$$u_i = -\nabla_{x_i} \Phi(e) = -\sum_{j \sim i} \left(\|e_k\|^2 - {d_k}^2 \right) e_k. \tag{4}$$

The closed loop dynamics can be written in state space form as

$$\dot{x} = -\mathcal{R}(x)x + R(x)^{\mathrm{T}} d. \tag{5}$$

A. Distance Error Dynamics

We now provide an alternative approach for the local stability analysis of the distance-constrained formation control in (5). Factorization of the dynamics in (5) yields

$$\dot{x} = -R(x)^{\mathrm{T}} \left(R(x)x - d \right). \tag{6}$$

Note that from (1) it can be seen that the expression $R(x)x - d$ is precisely the distance error defined in (2), i.e.,

$$\delta \triangleq R(x)x - d = \operatorname{diag}(e_i^{\mathrm{T}}) \underbrace{(E^{\mathrm{T}} \otimes I_2)x}_{e} - d. \tag{7}$$

As we are concerned with the behavior of the formation error, we now derive the formation error dynamics by differentiating (7) with respect to time,

$$\dot{\delta} = 2\operatorname{diag}(e_i^{\mathrm{T}})\dot{e} = 2\operatorname{diag}(e_i^{\mathrm{T}})(E^{\mathrm{T}} \otimes I_2)\dot{x}. \tag{8}$$

Combining (8) with (1) and (6) leads to the following expression for the formation error dynamics,

$$\begin{aligned} \dot{\delta} = f(\delta) &= -2R(x)R(x)^{\mathrm{T}}\left(R(x)x - d\right) \\ &= -2R(x)R(x)^{\mathrm{T}}\delta. \end{aligned} \tag{9}$$

B. Formation Stability Analysis

It is well known that the direct linearization of (5) around the target formation has multiple eigenvalues at the origin, and consequently cannot be analyzed by Lyapunov's indirect method [12]. In contrast, we now show that the linearization of the δ-dynamics in (9) leads to a Hurwitz state matrix, and thus local asymptotic stability is readily shown. In this direction, we first introduce the following assumption, which is widely used in the literature [8, 13].

Assumption 1. *Any framework $\mathcal{G}(x)$ satisfying the distance constraints $\{d_{ij}\}_{(i,j)\in\mathcal{E}}$ is minimally infinitesimally rigid.*

Theorem 1. *Under Assumption 1, the origin of the formation error dynamics (9) is locally asymptotically stable.*

Proof. Define the set $\Omega = \{x |\, R(x)x - d = 0\}$. For any $x^* \in \Omega$, $\delta = 0$ by definition, hence any $x^* \in \Omega$ corresponds to an equilibrium of (9). Denote $M(x) = R(x)R(x)^{\mathrm{T}}$. Evaluating the Jacobian of the dynamics (9) at the equilibrium $\delta = 0$ ($x = x^*$) gives

$$\begin{aligned} \left.\frac{\partial f(\delta)}{\partial \delta}\right|_{\delta=0,x=x^*} &= \left.\frac{\partial\left(-2M(x)\delta\right)}{\partial\delta}\right|_{\delta=0,x=x^*} \\ &= -2\left(\frac{\partial\left(M(x)\right)}{\partial\delta}\delta\right)\Bigg|_{\delta=0,x=x^*} - 2\left(M(x)\frac{\partial\delta}{\partial\delta}\right)\Bigg|_{\delta=0,x=x^*}. \end{aligned}$$

The linearized dynamics equation thus can be expressed as

$$\dot{\tilde{\delta}} = -2M(x^*)\tilde{\delta},$$

where $\tilde{\delta}$ is the variation of the state around the equilibrium point. From Assumption 1 and Corollary 1, it follows that $R(x^*)$ has full row rank, and therefore $M(x^*)$ is a symmetric positive-definite matrix. Thus, the equilibrium point $\delta = 0$ of the nonlinear formation error dynamics is locally asymptotically stable. □

The result of Theorem 1 shows that examining the linearized formation error dynamics allows for the use of Lyapunov's indirect method to show local asymptotic stabilization of the formation. In fact, exponential stability can also be shown using a similar approach as found in [13].

IV. Distance-Constrained Formation Tracking with Proportional Control

We now consider the formation controller in (5) and designate one agent as a leader. The leader is injected with an external reference velocity command, and the objective of the formation is to follow the leader while maintaining the specified inter-agent distances. Without the presence of any additional control, such a scheme will always lead to a steady-state error for the formation (i.e., $\lim_{t\to\infty} \|\delta(t)\| > 0$). This phenomena is demonstrated by a simple example shown in Figure 1(a). Here, 4 agents are tasked with maintaining a diamond shape formation (satisfying Assumption 1) while tracking the designated leader (marked in green). Figure 1(b) plots $\|\delta\|$ as a function of time, showing the steady-state error.

The addition of a velocity reference to the agent designated as a leader together with the control law in (4) leads to the following dynamics,

$$\dot{x} = -R(x)^{\mathrm{T}} \left(R(x)x - d\right) + Bv_{ref}. \tag{10}$$

Here, $B \in \mathbb{R}^{2n\times 2}$ is used to indicate which agent in the formation may receive the external velocity reference, $v_{ref} \in \mathbb{R}^2$ (i.e., if agent i is the leader, then the i-th block of B is I_2, and the remaining blocks are zero). The steady-state error in the formation can be bounded (and even eliminated) by introducing an appropriate stabilizing control into the control loop. A general control scheme is presented in Figure 2 and can be described as

$$\dot{x} = u + Bv_{ref}, \tag{11}$$

$$u = -R(x)^{\mathrm{T}} C\Big(R(x)x - d\Big), \tag{12}$$

where $C\Big(R(x)x - d\Big) = C(\delta)$, can be any stabilizing controller.

Before analyzing the stability of the control scheme proposed in (12), we first examine the performance of the formation with a leader. In particular, we show that for the dynamics in (12), assuming that C is a stabilizing controller, the velocity of the formation centroid will move at a velocity proportional to the reference, v_{ref}. In this direction, first define the centroid as

$$\bar{x} = \frac{1}{n}\sum_{i=1}^{n} x_i = \frac{1}{n}\left(\mathbf{1}_n^{\mathrm{T}} \otimes I_2\right) x. \tag{13}$$

Theorem 2. *Consider the system (11) and (12) and assume C is a stabilizing controller. Then the centroid of the formation, (13), moves at the constant velocity v_{ref}/n.*

Proof. Observe from (1) that $\left(\mathbf{1}_n^{\mathrm{T}} \otimes I_2\right) R(x)^{\mathrm{T}} = \left(\mathbf{1}_n^{\mathrm{T}} \otimes I_2\right)(E \otimes I_2)\mathrm{diag}(e_i) = 0$ due to the fact that $\mathbf{1}_n$ is the left null space of E. Using this property, we examine the dynamics of the centroid,

$$\dot{\bar{x}} = \frac{1}{n}\left(\mathbf{1}_n^{\mathrm{T}} \otimes I_2\right)\left(-R(x)^{\mathrm{T}} C(\delta) + Bv_{ref}\right) = \frac{1}{n}\left(\mathbf{1}_n^{\mathrm{T}} \otimes I_2\right) Bv_{ref}.$$

In the case that only one agent is being controlled (i.e., $(\mathbf{1}_n^{\mathrm{T}} \otimes I_2)B = I_2$), the centroid dynamics reduce to $\dot{\bar{x}} = v_{ref}/n$, concluding the proof. □

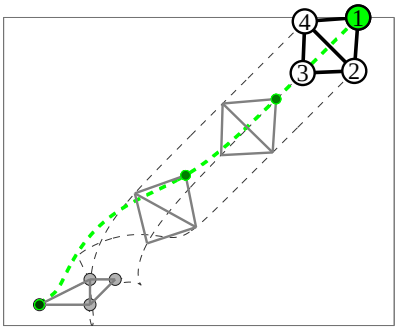

(a) An MIR formation tracking a leader.

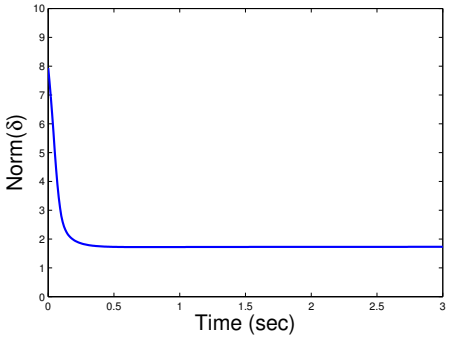

(b) A plot of $\|\delta\|$ showing a steady-state error.

Figure 1: Without any additional control, tracking a leader leads to a steady-state error in the formation.

Remark 1. *Note that the centroid does not actually track the reference velocity. However, if the number of agents in the ensemble is known by the leader, this is easily overcome by premultiplication of the reference velocity by the number of agents in the network.*

In the next subsection we propose a proportional gain control for the formation error controller C.

A. Proportional Gain Control

A *proportional controller* is a control loop feedback mechanism widely used in industrial control systems, and it is the first intuitive control gain that comes to mind when implementing a controller. A proportional controller generally operates with a steady-state error, sometimes referred to as droop. Droop may be mitigated by adding a compensating bias term to the set point or output, or corrected dynamically by adding an integral term (the latter will be discussed in the followup paper). The next equation describes a proportional controller that may be implemented as the controller C in (12),

$$u = -R(x)^{\mathrm{T}}(\kappa_P I_n)\left(R(x)x - d\right), \tag{14}$$

where κ_P is a scalar constant. Notice here that each agent utilizes the same gain parameter.

A proportional control system amplifies the error signal to generate the control signal. The closed-loop dynamics of the system utilizing the proportional control in (14) is thus

$$\dot{x} = R(x)^T(\kappa_P I_n)\left(R(x)x - d\right) + Bv_{ref}.$$

Examining the system from the error vector point of view will help to prove the stability of the origin. The dynamics of the formation error vector (7) with a proportional controller described in (14) can be derived as

$$\dot{\delta} \;\; = f(\delta, v_{ref}) = \;\; -2\kappa_P R(x)R(x)^T\delta + 2R(x)Bv_{ref}. \tag{15}$$

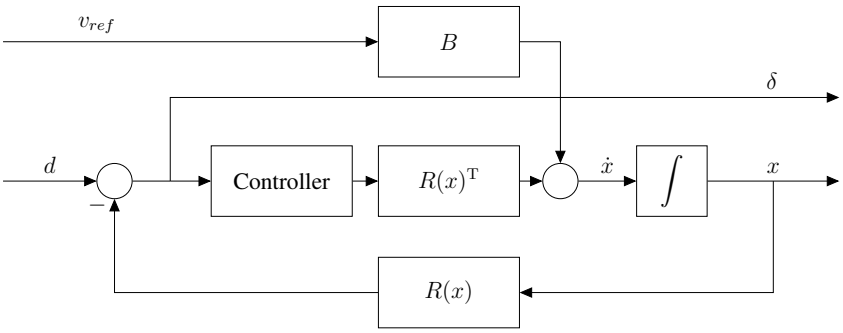

Figure 2: A formation control architecture for velocity tracking.

Theorem 3. *Under Assumption 1 and for any $\kappa_P > 0$, the origin of the zero-input $(v_{ref} = 0)$ error dynamics (15) is locally asymptotically stable.*

Proof. By using the same method described in Theorem 1, The linearized dynamics equation can be expressed as

$$\dot{\tilde{\delta}} = -2\kappa_P M(x^*)\tilde{\delta}\,,$$

where $\tilde{\delta}$ is the variation of the state around the equilibrium point. For any choice of $\kappa_P > 0$ the matrix $-2\kappa_P M(x^*)$ is Hurwitz (Because $M(x^*)$ is a symmetric positive-definite matrix) thus leading us to the local asymptotic stability of the equilibrium point $\delta = 0$ of the nonlinear formation error dynamics. □

Theorem 4. *In the local sense, under Assumption 1, and for any $\kappa_P > 0$, the error dynamics (15) is bounded input bounded output (BIBO) stable.*

Proof. The same actions are taken as in Theorem 1 in order to present the full linearized dynamics of (15). Define the set $\tilde{\Omega} = \{(x, v_{ref}) |\, f(x, v_{ref}) = 0\}$, which represents the equilibrium set of (15). We are interested in linearizing the system around a zero formation error, i.e., $\delta = 0$ and hence $x = x^*$ ($x \in \Omega$ as defined in Theorem 1). In this direction, define the set $\Omega_2 = \{(x, v_{ref}) |\, R(x)x - d = 0\,, f(x, v_{ref}) = 0\} \subset \tilde{\Omega}$. It then follows that any $(x, v) \in \Omega_2$ satisfies $x \in \Omega$ and $v = 0$. We now linearize our system around the point $(x^*, 0) \in \Omega_2$ to obtain the linear state space form [24]

$$\begin{aligned} \dot{\tilde{\delta}} &= \bar{A}\tilde{\delta} + \bar{B}\tilde{v} \\ y &= \bar{C}\tilde{\delta} + \bar{D}\tilde{v}, \end{aligned}$$

where $\tilde{\delta}$ is the variation of the state and $\tilde{v}$ is the variation of the input around the equilibrium point. The matrix $\bar{A}$ is obtained by evaluating the Jacobian of the dynamics (15) at the equilibrium $\delta = 0$ ($x = x^*$) and at the nominal input $v_{ref} = 0$:

$$\begin{aligned} \bar{A} = \left.\frac{\partial f(\delta, v_{ref})}{\partial \delta}\right|_{\delta=0, x=x^*, v_{ref}=0} &= \left.\frac{\partial \left(-2\kappa_P M(x)\delta + 2R(x)Bv_{ref}\right)}{\partial \delta}\right|_{\delta=0, x=x^*, v_{ref}=0} \\ &= -2\kappa_P M(x^*) + 2\left(\frac{\partial R(x)}{\partial \delta}Bv_{ref}\right)\Bigg|_{\delta=0, x=x^*, v_{ref}=0} \\ &= -2\kappa_P M(x^*) \end{aligned}$$

The Marix $\bar{B}$ represents the control matrix, and is obtained in a similar way:

$$\bar{B} = \left.\frac{\partial f(\delta, v_{ref})}{\partial v_{ref}}\right|_{\delta=0, x=x^*, v_{ref}=0} = 2R(x^*)B$$

The $\bar{C}$ matrix is the identity matrix reflecting the formation error vector as the output of the system with $\bar{D} = 0$. The complete linearized dynamics equation can be expressed as

$$\begin{aligned} \dot{\tilde{\delta}} &= -2\kappa_P M(x^*)\tilde{\delta} + 2R(x^*)B\tilde{v} \\ y &= \tilde{\delta} \end{aligned} \tag{16}$$

For a general linear system, the transfer functions matrix between the input and the output is given according to $G(s) = \bar{C}\left(sI - \bar{A}\right)^{-1}\bar{B} + \bar{D}$ [24]. The transfer function corresponding to the linearized dynamics (16) is thus

$$G(s) = \left(sI_m + 2\kappa_P M(x^*)\right)^{-1} 2R(x^*)B = 2\frac{adj\left(sI_m + 2\kappa_P M(x^*)\right)}{det(sI_m + 2\kappa_P M(x^*))}R(x^*)B. \tag{17}$$

BIBO stability can be concluded simply by examining the poles of $G(s)$, and those are obtained by solving the characteristic equation of $-2\kappa_P M(x^*)$. By Assumption 1, $M(x^*)$ is a symmetric positive-definite matrix, and therefore all of its eigenvalues are real and positive. Therefore, for positive κ_P, all the eigenvalues of $-2\kappa_P M(x^*)$ are located on the open left half plane and hence the system is BIBO stable. □

Owing to the structure of the matrices in the linearized dynamics, we are also able to provide an analytic expression for the steady-state error and also upper bounds that are expressed in terms of properties of the system.

Corollary 2. *Given a constant reference velocity* $\tilde{v} =$v *for the linearized dynamics in (16), the steady-state formation error is* $\lim_{t\to\infty}\tilde{\delta}(t) = \tilde{\delta}_{ss} = \frac{1}{\kappa_P}M(x^*)^{-1}R(x^*)B$v *and it is bounded as*

$$\left\|\tilde{\delta}_{ss}\right\| \leq \left|\frac{1}{\kappa_P}\right| \frac{\sqrt{d_{max}\cdot\lambda_{max}(L(\mathcal{G}))}}{\lambda_{min}(M(x^*))}\left\|\text{v}\right\|.$$

Proof. For a step input response of magnitude v we can use the final value theorem, since the eigenvalues of the dynamic matrix are all in the open left-half of the complex plane.

$$\begin{aligned} \lim_{t\to\infty}\tilde{\delta}(t) &= \lim_{s\to 0}\delta(s) = \lim_{s\to 0} s\frac{1}{s}G(s)\text{v} \\ &= \lim_{s\to 0}\left(sI_m + 2M(x^*)\kappa_P\right)^{-1} 2R(x^*)B\text{v} \\ &= \frac{1}{\kappa_P}M(x^*)^{-1}R(x^*)B\text{v}. \end{aligned}$$

Since $R(x^*)$ and $M(x^*)^{-1}$ are constant matrices, this immediately implies that for any bounded input the formation error will also be bounded. The euclidean norm of the formation error vector is considered in order to express the boundness of the steady-state error with the following norm inequalitiy

$$\left\|\tilde{\delta}_{ss}\right\| = \left\|\frac{1}{\kappa_P} M(x^*)^{-1} R(x^*) B\mathrm{v}\right\| \leq \left|\frac{1}{\kappa_P}\right| \left\|M(x^*)^{-1}\right\| \|R(x^*)\| \|B\| \|\mathrm{v}\|. \tag{18}$$

From the definition of B in (10), its norm is $\|B\| = 1$ and hence assigning a different agent with a reference velocity does not affect the boundness of the steady state error. Also observe that

$$\begin{aligned} \|M(x^*)\| &= \left\|R(x^*)R(x^*)^T\right\| \\ &= \left\|diag(e_i^{T*})(E^T \otimes I)(E \otimes I)diag(e_i^*)\right\| \\ &\leq \left\|diag(e_i^{T*})\right\| \left\|(E^T E \otimes I)\right\| \left\|diag(e_i^*)\right\|. \end{aligned} \tag{19}$$

The expression $E^T E$ is also known as $L_e(G)$, the edge Laplacian of a graph [25]. Using an SVD decomposition, the following equations hold,

$$\begin{aligned} \|E\| &= \sqrt{\lambda_{max}(E^T E)} = \sqrt{\lambda_{max}(L_e(\mathcal{G}))} \\ &= \sqrt{\lambda_{max}(E E^T)} = \sqrt{\lambda_{max}(L(\mathcal{G}))} \\ &= \left\|E^T\right\|. \end{aligned} \tag{20}$$

From the properties of the Kronecker product, The norm $\left\|(E^T E \otimes I)\right\|$ is equal to $\left(\left\|E^T E\right\| \cdot \|I\|\right)$, and hence $\left\|(E^T E \otimes I)\right\| = \|L_e(\mathcal{G})\|$. From (20) and since $L_e(\mathcal{G})$ is symmetric,

$$\|L_e(\mathcal{G})\| = \|L(\mathcal{G})\| = \lambda_{max}(L(\mathcal{G})). \tag{21}$$

Note also that

$$\begin{aligned} \left\|diag(e_i^{T*})\right\| &= \|diag(e_i^*)\| \\ &= \sqrt{\lambda_{max}\left[diag(e_i^{T*})\right]\left[diag(e_i^*)\right]} \\ &= \sqrt{\lambda_{max}\begin{bmatrix} \|e_1^*\|^2 & & \\ & \ddots & \\ & & \|e_m^*\|^2 \end{bmatrix}} \\ &= \sqrt{\max_k(d_k^2)} \triangleq d_{max}, \end{aligned} \tag{22}$$

where $\max_k(d_k^2)$ is the largest entry of the distance constraint vector d. From (19), (21) and (22) the upper bound of $\|M(x^*)\|$ is

$$\|M(x^*)\| \leq d_{max} \cdot \lambda_{max}(L(\mathcal{G})), \tag{23}$$

and as can be seen $\|M(x^*)\|$ depends on the structure of the graph. The matrix $M(x^*)$ is symmetric and hence $\|M(x^*)\| = \lambda_{max}(M(x^*))$. This fact will help us derive an upper bound to the norm of $R(x^*)$;

$$\|R(x^*)\| = \sqrt{\lambda_{max}\left[R(x^*)R(x^*)^T\right]} = \sqrt{\lambda_{max} M(x^*)} = \sqrt{\|M(x^*)\|}. \tag{24}$$

Combining (23) with (24) it can be concluded that

$$\|R(x^*)\| \leq \sqrt{d_{max} \cdot \lambda_{max}(L(\mathcal{G}))}. \tag{25}$$

Lastly, $\|M(x^*)^{-1}\|$ should also be bounded in order to completely bound the steady state error. The norm of the inverse of a matrix is related to its condition number. Denote $\gamma(M(x^*))$ as the condition number of a matrix $M(x^*)$, i.e., $\gamma(M(x^*)) = \frac{\lambda_{max}(M(x^*))}{\lambda_{min}(M(x^*))}$. By definition, $\gamma(M(x^*)) = \|M(x^*)\| \cdot \|M(x^*)^{-1}\|$, and hence

$$\left\|M(x^*)^{-1}\right\| = \frac{\lambda_{max}(M(x^*))}{\|M(x^*)\|\,\lambda_{min}(M(x^*))} = \frac{1}{\lambda_{min}(M(x^*))}. \tag{26}$$

By collecting (18), (25) and (26) the steady-state error can be bounded as

$$\left\|\tilde{\delta}_{ss}\right\| \leq \left|\frac{1}{\kappa_P}\right| \frac{\sqrt{d_{max} \cdot \lambda_{max}(L(\mathcal{G}))}}{\lambda_{min}(M(x^*))} \|\mathrm{v}\|, \tag{27}$$

and is affected both from properties of the structure of the graph, and from the largest entry of the distance constraint vector. □

Note that the value of the steady state error is found only in the local sense, and it is not the real steady state value but rather an approximation. This is due to the fact that the matrices $R(x^*)$ and $M(x^*)^{-1}$ are computed around the equilibrium points, which accure when δ is strictly zero.

While Theorem 3 provides us with information about the stability of the autonomous system with a positive κ_P, here an additional condition on κ_P is provided in the context of error boundness. Explicitly, the upper bound will become smaller as κ_P gets higher.

By introducing a stabilizing proportional gain controller into the formation control scheme we were able to accomplish the task of reducing the formation tracking error. Some graph features affect the results of this section directly or indirectly. Firstly, for a constant reference velocity, the centroid moves at a constant velocity proportional to the number of the agents in a graph. Secondly, the steady state error has an upper bound related directly to the Laplacian eigenvalues. The location of the those eigenvalues can be correlated to the graph structure, and therefore used to identify desirable and undesirable formation interconnection topologies.

V. Simulations

We now demonstrate the results of Theorem 4 and Corollary 2 with a numerical example. Consider two minimally infinitesimally rigid frameworks with 6 agents as illustrated in Figure 3. The graph in Figure 3(a) has $\lambda_{max}(L(\mathcal{G})) = 6$ while the graph in Figure 3(b) has $\lambda_{max}(L(\mathcal{G})) = 5.343$. In order to know how the steady state error is affected by different types of graphs, the mobile agents are driven by the dynamics in (11) under control law (14) and are initialized with arbitrary positions and zero velocities. We would expect a graph with a lower $\lambda_{max}(L(\mathcal{G}))$ to yield a smaller upper bound, according to Corollary 2.

The desired inter-agents distances were chosen such that the target formation will have the same geometric shape, and are labeled above the edges of each graph in Figure 3. Also, only the green colored agent is injected with a reference velocity, with a magnitude of $0.2[m/sec]$.

The motion of the agents is illustrated in Figure 4 in which the initial positions are marked with grey circles and the final positions (at t_{final}) with numbered circles. The dashed lines are the trajectories of each agent and the proportional controller gain was initially set to $\kappa_P = 2$.

Figure 5 describes the norm of the true error, δ. It can be seen that the steady state error indeed closely matches the linearized steady state value, marked in a green dashed line, as it is

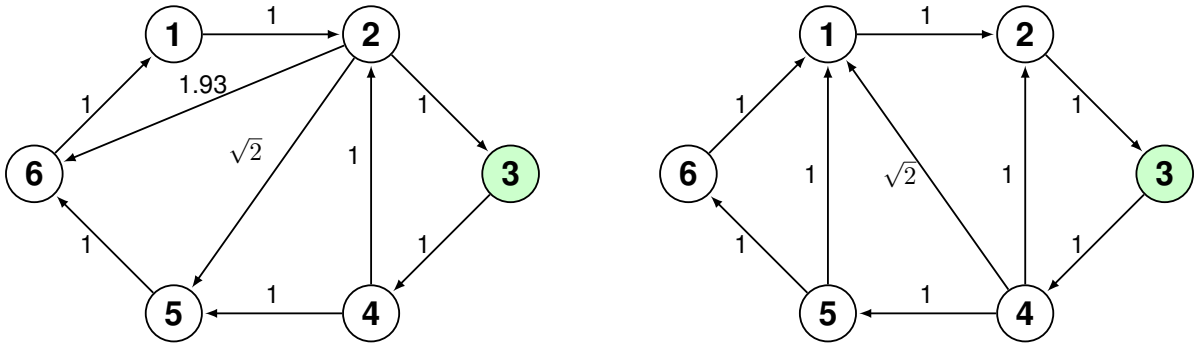

(a) Graph 1.

(b) Graph 2.

Figure 3: The distance constraint vector d as it is presented graphically on a two types of graphs.

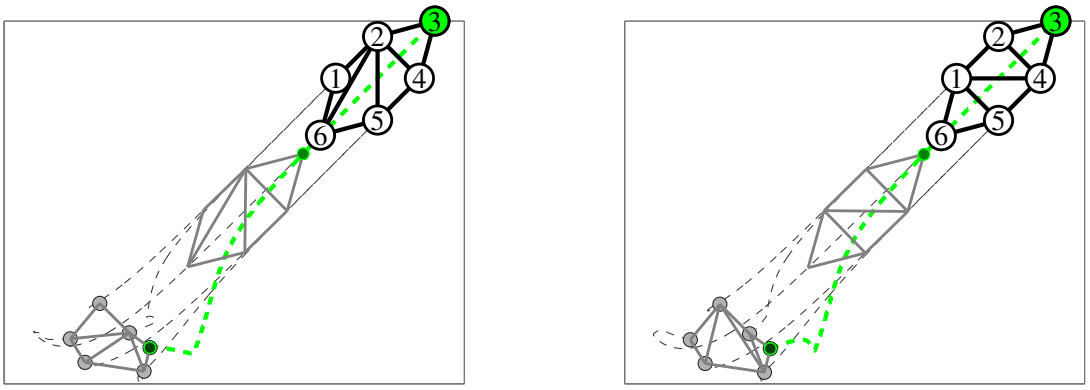

(a) Agents trajectories according to Figure 3(a).

(b) Agents trajectories according to Figure 3(b).

Figure 4: A MIR formations tracking a leader.

derived from (18). As a comparison, the true steady state value of Figure 5(a) is $\delta_{ss} = 0.0411$ while the steady state value from Figure 5(b) is $\delta_{ss} = 0.0418$. Sharp-eyed readers may see that although the bound of $Graph\,2$ is smaller than that of $Graph\,1$, the simulation actually shows a smaller steady state error for $Graph\,1$. That is due to the fact that the bound is not tight and is only an approximation which was derived from the linearized version of the non-linear system.

In line with the expectations, smaller $\lambda_{max}(L(\mathcal{G}))$ does cause the upper bound to be smaller, but this does not promise us that is how it will be for other types of graphs. The combination of $\lambda_{max}(L(\mathcal{G}))$, $\lambda_{min}(M(x^*))$, and d_{max} should be considered as a whole in order to examine this bound accurately. In this example the framework in Figure 4(a) has $\lambda_{min}(M(x^*)) = 0.57$ and the framework in 4(b) holds $\lambda_{min}(M(x^*)) = 1.996$ which according to Corollary 2 affirms the correctness of the results. Lastly, as κ_P increases, the steady state formation error gets smaller. This can be observed by the norm of the error for different values of κ_P in Figure 6.

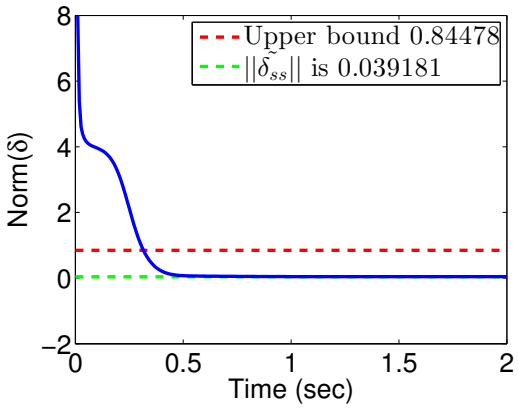

(a) The formation error norm, $\|\delta\|$, in correspondence to the formation in Figure 3(a).

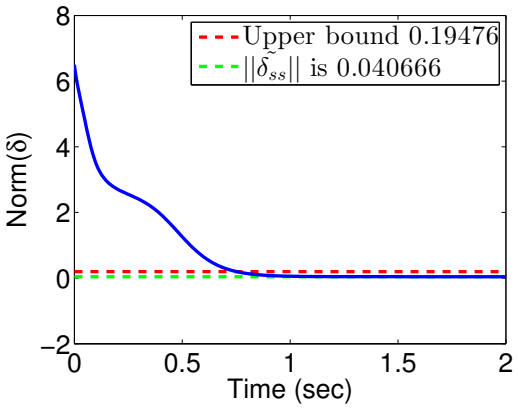

(b) The formation error norm, $\|\delta\|$, in correspondence to the formation in Figure 3(b).

Figure 5: The norm of the formation tracking error with an upper bound

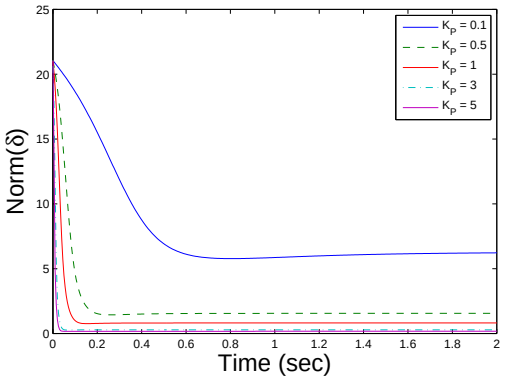

Figure 6: Norm of the formation error for different κ_P gain values..

VI. Conclusion

In order to solve the velocity tracking problem of a multi-agent system, we introduced a distance-based rigidity control law combined with a proportional control scheme on the formation error. We showed that the formation error vector elements are reduced as the gain of the controller increases, and that the formation tracks the controlled agent with the reference velocity. We also show that the boundness properties of the steady state error (and in the future even disturbance rejection and other measures of interest) are correlated to the Laplacian eigenvalues, and thus to the graph structure. In future work we will show that the formation error can be eliminated completely by introducing integral action.

Acknowledgements

The work presented here has been supported by the Israel Science Foundation.

References

[1] R. Olfati-Saber and R. M. Murray, "Graph rigidity and distributed formation stabilization of multi-vehicle systems," in *41st IEEE Conference on Decision and Control*, vol. 3, 2002, pp. 2965–2971.

[2] D. Zelazo, A. Franchi, F. Allgöwer, H. H. Bülthoff, and P. R. Giordano, "Rigidity maintenance control for multi-robot systems." in *Robotics: Science and Systems*, 2012.

[3] B. Anderson, C. Yu, B. Fidan, and J. Hendrickx, "Rigid graph control architectures for autonomous formations," *IEEE Control Systems Magazine*, vol. 28, no. 6, pp. 48–63, 2008.

[4] B. Anderson, B. Fidan, C. Yu, and D. Walle, "UAV formation control: Theory and application," in *Recent Advances in Learning and Control*, 2008, pp. 15–33.

[5] M. A. Belabbas, "On global feedback stabilization of decentralized formation control," in *50th IEEE Conference on Decision and Control and European Control Conference*, 2011, pp. 5750–5755.

[6] D. V. Dimarogonas and K. H. Johansson, "On the stability of distance-based formation control," in *47th IEEE Conference on Decision and Control*, 2008, pp. 1200–1205.

[7] T. Eren, P. N. Belhumeur, B. D. Anderson, and A. S. Morse, "A framework for maintaining formations based on rigidity," in *15th IFAC World Congress*, Barcelona, Spain, 2002, pp. 2752–2757.

[8] L. Krick, M. E. Broucke, and B. A. Francis, "Stabilization of infinitesimally rigid formations of multi-robot networks," *International Journal of Control*, vol. 82, no. 3, pp. 423–439, Mar. 2009.

[9] D. Zelazo, A. Franchi, H. H. Bulthoff, and P. Robuffo Giordano, "Decentralized rigidity maintenance control with range measurements for multi-robot systems," *The International Journal of Robotics Research*, vol. 34, no. 1, pp. 105–128, Nov. 2014.

[10] L. Asimow and B. Roth, "The rigidity of graphs," *Transactions of the American Mathematical Society*, vol. 245, pp. 279–289, November 1978.

[11] A. Y. Alfakih, "On the dual rigidity matrix," *Linear Algebra and its Applications*, vol. 428, no. 4, pp. 962–972, 2008.

[12] L. Krick, "Application of graph rigidity in formation control of multi-robot networks," Ph.D. dissertation, University of Toronto, 2007.

[13] F. Dörfler and B. Francis, "Formation control of autonomous robots based on cooperative behavior," in *IEEE European Control Conference*, Budapest, Hungary, 2009, pp. 2432–2437.

[14] L. Fang and P. J. Antsaklis, "Decentralized formation tracking of multi-vehicle systems with nonlinear dynamics," in *14th Mediterranean Conference on Control and Automation*, 2006, pp. 1–6.

[15] M. Egerstedt, "Formation constrained multi-agent control," *IEEE Transactions on Robotics and Automation*, vol. 17, no. 6, pp. 947–951, 2001.

[16] H. Su, X. Wang, and W. Yang, "Flocking in multi-agent systems with multiple virtual leaders," *Asian Journal of control*, vol. 10, no. 2, pp. 238–245, 2008.

[17] H. Su, X. Wang, and Z. Lin, "Flocking in multi-agent systems with a virtual leader," *IEEE Transactions on Automatic Control*, vol. 54, no. 2, pp. 293–307, 2009.

[18] H. G. Tanner, A. Jadbabaie, and G. J. Pappas, "Flocking in fixed and switching networks," *IEEE Transactions on Automatic Control*, vol. 52, no. 5, pp. 863–868, 2007.

[19] R. Olfati-Saber, "Flocking for multi-agent dynamic systems: Algorithms and theory," *IEEE Transactions on Automatic Control*, vol. 51, no. 3, pp. 401–420, 2006.

[20] H. G. Tanner, A. Jadbabaie, and G. J. Pappas, "Stable flocking of mobile agents part i: Dynamic topology," in *42nd IEEE Conference on Decision and Control*, vol. 2, 2003, pp. 2016–2021.

[21] C. Godsil and G. Royle, "Algebraic graph theory," *Springer*, 2001.

[22] T. Tay and W. Whiteley, "Generating isostatic frameworks," *Structural topology*, vol. 11, pp. 21–69, 1985.

[23] D. V. Dimarogonas and K. H. Johansson, "Stability analysis for multi-agent systems using the incidence matrix: Quantized communication and formation control," *Automatica*, vol. 46, no. 4, pp. 695–700, April 2010.

[24] K. Ogata, "Modern control engineering fourth edition," *Upper Saddle River: Prentice Hall*, 2002.

[25] D. Zelazo, A. Rahmani, and M. Mesbahi, "Agreement via the edge laplacian," in *46th IEEE Conference on Decision and Control*, 2007, pp. 2309–2314.